IJIE

INTERNATIONAL JOURNAL OF INTEGRATED ENGINEERING
ISSN: 2229-838X e-ISSN: 2600-7916

Vol. 18 No. 2 (2026) 167-181
https://publisher.uthm.edu.my/ojs/index.php/ijie

Evaluation of a Passive Direct Greenhouse Solar Dryer under Varying Load Conditions

Abdul Rahman[1], Mohd Suffian Misaran[1]*, Chu Chi Ming[1], Rachel Fran Mansa[1], Tham Heng Jin[1], Mohd Adzrie Radzali[1], Mohd Kamel Wan Ibrahim[1], Md. Mizanur Rahman[2]

[1] *Faculty of Engineering,*
Universiti Malysia Sabah (UMS), Kota Kinabalu, Sabah, 88400, MALAYSIA
[2] *Department of Mechatronics Engineering,*
World University of Bangladesh, 151/8, Green Road, Dhaka, 1205, BANGLADESH

*Corresponding Author: suffian@ums.edu.my
DOI: https://doi.org/10.30880/ijie.2026.18.02.014

Article Info

Received: 15 November 2025
Accepted: 20 March 2026
Available online: 28 April 2026

Keywords

Greenhouse solar dryer, sponge, passive dryer, solar energy, natural convection

Abstract

This study evaluates the thermal and drying performance of a passive direct greenhouse-type solar dryer using synthetic sponge as a controlled model for porous biological materials. Sponge was selected to eliminate the variability in size, porosity, and initial moisture content typical of agricultural products and thereby isolate the effects of load density and spacing on heat–mass transfer. Experiments were conducted over three days. Experimental data such as solar irradiance, temperature profiles, and drying kinetics were recorded while open-sun drying (OSD) act as control. Average solar irradiance ranged from 657–734 W m^{-2}, while drying efficiencies of the passive system varied between 76–86%, substantially exceeding OSD (≈ 30%). On Day 1, 5-inch inter-sponge spacing produced the highest chamber temperature (43.25 °C) but less uniform moisture removal. In contrast, 1-inch spacing on Day 3 enhanced thermal stratification (ΔT ≈ 17.5 °C) and yielded quantitatively uniform drying across trays. The final moisture ratios of top 0.004 (99.6% removed), middle 0.110 (89.0%), and bottom 0.067 (93.3%). Findings show that inter-sponge spacing critically governs convective heat transfer and internal heat retention. It demonstrates that passive greenhouse dryers can maintain high efficiency and near-uniform drying under moderate solar input. Based on the airflow–thermal response, it is recommended to have tight lateral inter-piece spacing (~1 inch) to increase vapor residence time and internal heat retention. Also, used in conjunction with the T-shaped enclosure's continuous roof outlets (0.4 m × 2.5 m) and four low-level inlets (0.1 m above floor) to reinforce buoyancy-driven natural convection without active fans.

1. Introduction

Drying is a fundamental process that is defined as the removal of water or any other solvents from any substance by evaporation, mainly from solid, semi-solid, or liquid materials. Drying is a vital process for various industries, particularly in agriculture, food, pharmaceutical, and materials industries. The importance of drying is associated with its ability to increase the shelf life of any product by preventing microbial growth, reducing weight for transportation, and facilitating convenience in storage [1], [2]. This process can be achieved through various methods, each with different energy requirements, impacts on the material and drying kinetics.

Drying techniques can be classified into natural drying techniques and artificial drying techniques. Natural drying techniques mostly involve the usage of environmental parameters for drying and open sun as natural drying technique mostly used due to its ease of operation and relatively low operating cost [3]-[5]. However, it is highly weather-dependent and vulnerable to drying contamination, uneven drying rates, long drying times, and nutrient loss [6]. Artificial methods such as convective drying, freeze drying, and microwave drying offer greater control and efficiency but often require substantial energy input and infrastructure [7]-[10]. Solar drying has emerged as a sustainable alternative, leveraging renewable solar energy to achieve effective moisture removal with minimal environmental impact over traditional drying [11], [12]. Solar drying systems are designed to overcome the limitations of traditional drying. While, a more controlled version of sun drying, utilize solar radiation more effectively, often incorporating protective features against environmental elements, thus improving food quality and drying efficiency [13], [14].

Solar dryers are classified into hybrid and non-hybrid (Solar dryer), active and passive, direct, indirect, and mixed-mode systems. Hybrid solar dryers combine solar energy with other energy sources like electricity, biomass, or thermal energy storage to improve drying performance and non-hybrid utilize solar energy [4]. Furthermore, Passive solar dryers utilize natural air movement (natural convection) to circulate air, while active solar dryers use forced air movement (forced convection) [11]. In addition, Direct solar dryers expose the product to sunlight within a transparent enclosure, while indirect dryers use solar collectors to heat air that is then circulated over the material. Mixed-mode dryers combine both approaches to optimize drying performance [15]. Moreover, solar dryers can be categorized over design and material used [16]. Greenhouse solar dryers could be a hybrid or non-hybrid, active or passive, direct and mixed mode due to his transparent structure. For instance, a hybrid active mixed-mode solar dryer used by a researcher to dry crops [17]. Various solar dryer has been extensively studied for agricultural products like tomatoes [18], mushrooms [19], and peppers [20].

Therefore, the objective of the present study is to evaluate the performance of a novel T- shaped passive direct greenhouse solar dryer with different tray load densities and inter-spacing arrangements using synthetic sponges as the drying material. In the present study, the performance parameters considered are drying kinetics, temperature distribution, moisture removal characteristics, and the effect of loading arrangements on drying uniformity. The study will determine the best loading conditions that would balance the drying efficiency and uniformity of the loading conditions by the systematic increase of tray load density which automatically leads to the decrease of inter-spacing. This study directly supports broader sustainability goals by promoting renewable energy based drying solutions that reduce dependence on fossil fuel heating, lower operational emissions, and enhance food processing resilience in humid tropical regions. By improving passive natural convection performance, the work contributes to scalable, low carbon post-harvest technologies aligned with sustainable development priorities.

W_1	Initial weight of water in sponge, kg
W_2	Final weight of water in sponge after drying interval, kg
OSD	Open Sun Drying
Q_{sol}	Total quantity of heat supplied to the dryer, kJ
Q_e	Energy utilized for moisture evaporation, kJ
M_w	Mass of water removed during drying, kg
λ	Latent heat of vaporization of water, $kJ \cdot kg^{-1}$
η	Drying system efficiency, %
A	Aperture / exposed solar collection area, m^2
I	Solar irradiance, $W \cdot m^{-2}$
t	Drying duration / exposure time, s
ΔW	Mass of water removed between two-time intervals, kg
DR	Drying rate, $kg \cdot h^{-1}$
Δt	Time difference between measurements, h
MR	Moisture Ratio
M_t	Moisture content at time t, kg water/kg dry matter
M_i	Initial moisture content, kg water/kg dry matter
T_{layer}	Temperature measured at a specific tray level (1–5), °C
Tout	Outlet air temperature, °C

Int. Journal of Integrated Engineering Vol. 18 No. 2 (2026) p. 167-181

T_{amb}	Ambient temperature, °C
ΔT	Vertical temperature difference (e.g., between L1 and L5), °C
RH	Relative humidity, %
v_w	Ambient wind speed (from anemometer), $m \cdot s^{-1}$
G	Solar radiation (pyranometer reading; alternative to I), $W \cdot m^{-2}$
S	Inter-sponge spacing (1 inch, 3-inch, 5 inch), in
N	Number of sponges per tray (load density)
A_{tray}	Area of drying tray, m^2
H_{in}	Height of inlet opening, m
H_{out}	Height of outlet / roof vent, m
$\dot{m}_{air}$	Air mass flow rate (qualitatively inferred; smoke-test based), $kg \cdot s^{-1}$
ρ_{air}	Density of air, $kg \cdot m^{-3}$
C_p	Specific heat capacity of air, $kJ \cdot kg^{-1} \cdot K^{-1}$
SMER	Specific Moisture Extraction Rate, $kg \cdot kWh^{-1}$

2. Structure Materials and Method

Section 2 outlines the materials, experimental setup, and procedures used to evaluate the performance of the passive T-shape greenhouse solar dryer. These methods were selected to provide controlled and repeatable measurements of thermal behavior, airflow distribution, and drying kinetics under varying loading and spacing configurations.

2.1 Description of the T-shape Solar Dryer

The Faculty of Engineering at Universiti Malaysia Sabah developed and patented a T-shaped passive solar dryer (Application No.: PI-2022005388, 2022) as shown in Fig. 1 that improves the natural convection by using a chimney-like "T" shape. The T-shaped roof forms a transverse low-pressure plenum that augments the stack effect, increasing buoyancy-driven mass flow through all three columns while minimizing short-circuiting near upper trays. The paired continuous outlets (0.40 m × 2.50 m each) lower exhaust resistance and stabilize the pressure field, promoting more uniform vertical draw across columns without fans. The initial design used 200g of short fibre material in laboratory tests. Subsequently, it scaled up by 1:2.5 to allow bulk drying of a large number of trays without changing the T-shape. The dryer has a length, width, and height of 2.5 m x 1.5 m x 2.3 m, and total wall as well as aperture area of 25.66 m^2 and 3.75 m^2 respectively. The drying chamber is equipped with three columns with 5 layer each. Each tray has 0.91 m^2 drying area and constructed of PVC-coated galvanized iron wire mesh (10 mm x 10 mm openings, 1.2 mm wire diameter).

Subsequently, the trays 0.3-0.4 m above the ground and spacing between trays is 0.3 m. The air is introduced to the dryer via four inlets that are 0.1 m above the ground level on either side of the dryer, and the air is released through continuous roof outlets (0.4 m x 2.5 m). The enclosure is clad with 200 μm UV-stabilized polyethylene (PE) greenhouse film (transparent), selected for high solar transmittance and durability in tropical exposure. The incline edges of T shape help to drain and prevent the entry of rainwater to chamber. A fine wire mesh (0.8 mm x 0.8 mm, 0.16 mm thick) is installed at the outlets and inlets to keep out debris, insects and especially cold inflow from exhaust. The dryer is oriented to the south to take the advantage of maximum solar energy consumption according to Malaysian latitude.

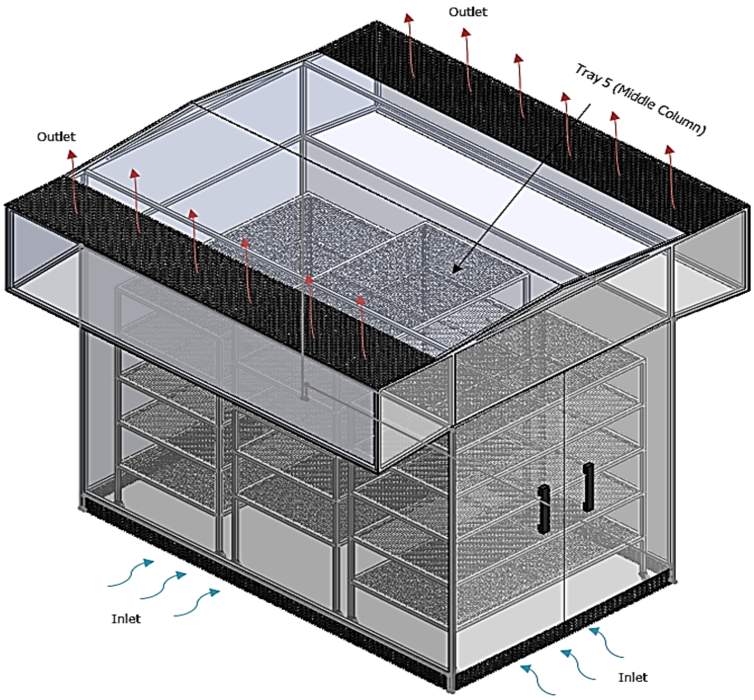

Fig. 1 *Schematic diagram of the developed solar dryer showing the air inflow and outflow pathways*

2.2 Airflow Visualization Test (Smoke Test)

A smoke flow test was conducted to qualitatively visualise the internal airflow behaviour in the developed greenhouse solar dryer and to characterise the possible air leakage areas. Smoke was produced with burning egg trays near to inlet. The movement of smoke was observed visually distance to determine the direction of airflow, the flow paths and the relative distribution of air among tray levels towards the outlet. This smoke test was only used as a qualitative assessment process rather than to measure airflow quantitatively.

2.3 Preparation of Raw Material

This research is based on drying systems to dry agricultural commodity in high humid conditions of tropical regions. There are a number of challenges that possibly arise in carrying out controlled experiments using real biological materials such as the size, shape, porosity and the initial moisture content of agricultural products vary considerably and may introduce experimental variability and influence the uniformity in the performance evaluation.

Synthetic sponge was selected as a controlled, repeatable surrogate to evaluate airflow–temperature coupling and drying kinetics without the confounding variability typical of biological commodities (e.g., heterogeneous geometry, porosity, and initial moisture content). Sponge is well investigated as open cell porous material with uniform pore connectivity and consistent uptake/release of water, which enables us to be able to isolate the influence of inter-sponge spacing and load density to the convective heat transfer and moisture removal. At the transport level, sponge also has the same governing processes that control drying of porous biological materials-capillary-driven redistribution of liquids, vapor diffusion through connected pores and surface convection of fluids. These mechanisms are captured in canonical porous media drying theory and validated at various model systems (capillary/vapor diffusion regimes, constant rate and falling rate periods) [21], [22]. Experiments on cellulose and polymer sponges demonstrate capillary imbibition and pore scale evolution consistent with food and plant tissues: early Washburn type wetting followed by structure dependent transport transitions, and poro elasto capillary effects that control liquid pathways and drying front motion [23], [24].

The sponge mattress was obtained from a local market in Kota Kinabalu, Sabah, Malaysia. It was then cut into square shapes of size 6-inch x 6 inch with a fixed thickness of 1 inch. Before the commencement of the experiments, the sponges were dried under the sun to eliminate any traces of moisture. The average weight (7.1 g) of per dry sponge was recorded. Prior to experiment, the sponges were immersed in water and then excess water on the sponge surfaces was manually removed through squeezing with uniform pattern. The weight of the wet sponges was recorded before being placed on the drying trays (three sponge pieces weighted together because it arranged and incremented 3 per row on tray). Throughout the experimental period, consistent pattern and procedure was maintained to achieve uniform conditions. The process of preparation material was shown in Fig. 2. In addition to that every 2-hour sponge weight were recorded for drying evaluation.

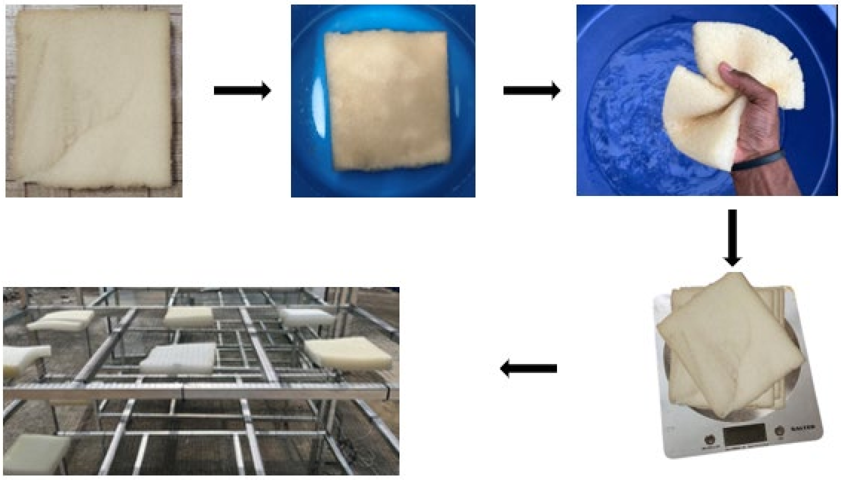

Fig. 2 *Step by step preparation of sponge samples for drying*

2.4 Sampling Strategy

The thermal behaviour of the dryer was monitored using DHT22 sensors installed in all three columns at the first and fifth tray levels, allowing quantification of the vertical temperature gradient throughout the drying chamber. Sample mass was recorded every two hours using an electronic balance, taken from the first, third, and fifth tray levels of the front column. This column was selected because space constraints limited access to all columns and because frequent handling could disrupt airflow during drying.

Representativeness of this sampling approach was verified through two independent indicators. First, the symmetrically placed inlets (0.10 m above the floor) and continuous roof outlets ensured the three columns received equivalent airflow. Correspondingly, DHT22 measurements from Layers 1 and 5 showed consistent thermal responses across all columns throughout the trials. Second, smoke-flow visualization confirmed uniform upward convection with no recirculation zones or preferential bypass between columns. Given this symmetric airflow design and corroborating sensor and smoke-test evidence, gravimetric measurements from the front column were taken as representative of chamber-wide drying behaviour.

2.5 Performance Metrics and Calculation Methods

The performance of the solar dryer was assessed using standard drying kinetics and energy-based indicators. The mass of water removed during each interval was first determined from the change in sample mass between two consecutive measurements, as defined in Eq. (1):

$$\Delta W = W_{t,1} - W_{t+\Delta t,2} \tag{1}$$

Drying efficiency (η) represents the proportion of available solar energy that is effectively used for moisture evaporation. It is calculated using the ratio of the energy required to evaporate water to the incident solar energy received by the dryer, as expressed in Eq. (2):

$$\eta = \frac{Q_e}{Q_{sol}} = \frac{M_w \lambda}{A \times I \times t} \times 100 \tag{2}$$

The drying rate quantifies the rate at which moisture is removed from the material during each interval. It is obtained by dividing the mass of water lost by the duration of the interval, as shown in Eq. (3):

$$DR = \frac{\Delta W}{\Delta t} \tag{3}$$

Moisture ratio (MR) is a dimensionless parameter used to describe the progression of drying by comparing the instantaneous moisture content to the initial moisture content. It is defined in Eq. (4):

$$MR = \frac{M_t}{M_i} \tag{4}$$

The MR decreases from 1 at the start of drying toward 0 as the product approaches equilibrium moisture. Because MR normalizes moisture content, it allows meaningful comparison of drying behavior across different loadings or operating conditions. Tracking MR and DR over time enables the development of drying curves, which were used to evaluate drying kinetics and compare the performance of the different spacing configurations tested in this study.

2.6 Instruments Used During the Experiment

Digital temperature and humidity sensor (DHT22) was used to measure the temperature and relative humidity at various locations in the solar dryer such as in the drying chamber, the plane center of dual continues exit airflow path and externally to monitor ambient conditions. Its accuracy and stability made it possible to monitor the drying environment continuously. To measure the speed of wind outside, a three-cup anemometer (Cytron Technologies) was installed. The Hukseflux pyranometer was used to measure incident solar irradiance on the collector surface; this parameter is necessary to estimate the available solar energy and relate it with the drying efficiency. The weight of the sample at the various drying stages was recorded using a Salter electronic weighing balance, which gives accurate mass data necessary to calculate the percentage of moisture extracted and the drying rate. Moreover, the sensors were connected to an Arduino-based data acquisition system with SD card storage. All the instruments were used as tabulated in Table 1.

Table 1 *Instrument used in experiment*

No.	Instrument	Model / manufacturer	Measurement parameter	Range / accuracy
1	Digital temperature & humidity sensor	DHT22 (AM2302)	Temperature (°C), relative humidity (%)	–40 to 80 °C (±0.5 °C); 0–100 % RH (±2 %)
2	Cup anemometer	Cytron 3-cup anemometer	Ambient wind speed (m/s)	0.3–30 m/s (±0.3 m/s)
3	Pyranometer	Hukseflux LP02 / equivalent	Solar irradiance (W/m^2)	0–2000 W/m^2 (±5 %)
4	Digital weighing scale	Salter	Sample mass (kg)	0–50000 g (±0.1 g)
5	Data logging and IoT platform	Arduino + thing speak	Data acquisition & transmission	Real-time logging

2.7 Sensor Placement for Experimental Measurements

The sensor arrangement used in the experiment is presented in Fig. 3. In each column, there was one sensor located at Layer 1 and another at Layer 5, about 50 mm above the tray surface and at the plan-wise center. These locations were chosen to measure the vertical temperature and humidity gradient between the lowest and highest level on the tray without obstructing airflow. To monitor exhaust conditions, additional DHT22 sensors were installed at the center of each roof outlet (left and right). Ambient reference measurements were obtained from a DHT22 sensor placed 1.5 m upwind of the dryer, alongside a pyranometer for solar irradiance and an anemometer for ambient wind speed. Layers 2–4 were intentionally left uninstrumented to avoid disturbing the natural convection pattern inside the chamber.

Int. Journal of Integrated Engineering Vol. 18 No. 2 (2026) p. 167-181

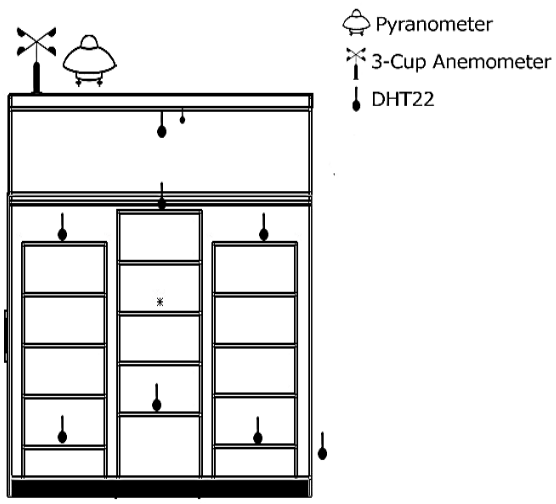

Fig. 3 *Sensor placement for experimental measurements in the solar dryer*

3. Results and Discussion

The drying efficiency of the solar dryer was experimentally evaluated for passive system under different weather and loading conditions. Three configurations tested, day one 12 pc of sponge/tray with five-inch gap between two sponge, day two 15 pc of sponge/tray with one inch distance and third day 18 pc of sponge/tray tested with one inch distance between them. In parallel, open sun drying tested as shown in Fig. 4. The number of sponges and space between them for open sun equal to number of sponges/ trays. one configuration tested one day. These series of experiment took place in Universiti Malaysia Sabah 14-21 September 2025 from 9 am to 3 pm. The weight of one sponge is 7.12 g and dimension is 6inch x 6inch with 1 inch thickness. The developed solar dryer is shown in Fig. 4. Solar dryer can adjust 3 vertical columns, and one column consists of 5 layers. Each tray/per column area is equal to OSD footprint area. Dryer is tested with full capacity, but drying efficiency is done using bottom, middle and top tray of front columns. Assumed that air flow is uniform within dryer at same level. Therefore, each column expected to show same performance.

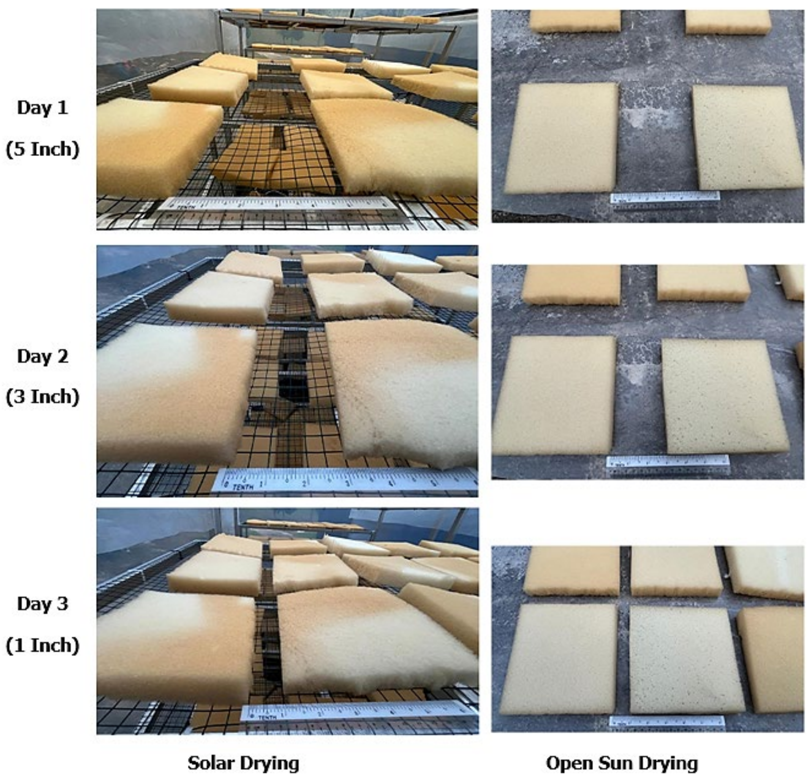

Fig. 4 *Arrangement of sponge samples showing load density and spacing between sponges*

3.1 Airflow Distribution Analysis Using Smoke Test

A smoke test was conducted to examine the airflow from inlets to outlets and to verify the internal circulation pattern of the solar dryer, as shown in Fig. 5. This technique is useful in identifying stagnant area or short-circuiting of airflow that may affect drying performance. In this test, a small amount of non-toxic smoke, produced by burning egg trays, is introduced into the inlet of the solar dryer, and its movement is monitored to determine how air passes through the drying chamber and interacts with the trays and exits through the roof vents.

The smoke plume consistently rose towards the outlets, showing that there is a strong buoyancy-driven natural convection current in the solar dryer. Moreover, this confirms that there is an effective airflow route from inlets to outlets throughout all tray levels in the drying chamber. Moreover, the smoke plume pattern changed depending on the density of the loaded trays in the drying chamber. For instance, on Day 1, there is a wider spacing of trays in the drying chamber, resulting in a broader and slower-moving smoke plume since the vertical temperature gradient is small (7-15 °C). In contrast, on Day 3, there is a dense 1-inch spacing of trays in the drying chamber, resulting in a faster-moving smoke plume since there is a higher thermal stratification in the drying chamber (ΔT = 17 °C).

Fig. 5 *Illustration of smoke analysis of developed solar dryer*

3.2 Thermal Distribution of Passive Greenhouse System

The thermal distribution inside the passive greenhouse solar dryer was evaluated to understand how solar irradiance, airflow behavior, and loading configurations influenced temperature patterns across the drying chamber. These thermal characteristics are essential for interpreting drying performance, uniformity, and energy utilization under the three experimental conditions.

3.2.1 Temperature and Solar Radiation Profiles

The solar irradiance temperature profile for days 1 to 3 is shown in Fig. 6. On day 1, solar irradiance levels ranged from a minimum of 516 W/m^2 to a maximum of 903.46 W/m^2, with an average of approximately 734 W/m^2. The temperature levels in Layer 1 ranged from 33.60 °C to 37.83 °C, and the average chamber temperature peaked at 43.25 °C. The outlet temperature also peaked at its maximum value at a solar irradiance of 903.46 W/m^2.

For day 2, solar irradiance levels ranged from a minimum of 444.33 W/m^2 to a maximum of 959.08 W/m^2, with an average of approximately 711 W/m^2. The temperature levels in Layer 1 ranged from 31 °C to 36 °C, whereas Layer 5 temperature levels ranged from 34 °C to 44 °C. This indicates a consistent increase in temperature from Layer 1 to Layer 5 due to solar irradiance. The average chamber temperature peaked at 40 °C at a solar irradiance of 959.08 W/m^2, which is the maximum solar irradiance level. The maximum outlet temperature recorded was 47 °C.

On day 3, solar irradiance levels ranged from a minimum of 320 W/m^2 to a maximum of 1,018.21 W/m^2, with an average of approximately 657 W/m^2. The temperature levels in Layer 1 ranged from 28.83 °C to 36.68 °C, whereas Layer 5 temperature levels ranged from 34.43 °C to 46.35 °C. The average chamber temperature peaked at 41.52 °C at a solar irradiance of 1,018.21 W/m^2, which is the maximum solar irradiance level. The maximum outlet temperature recorded was 47.05 °C.

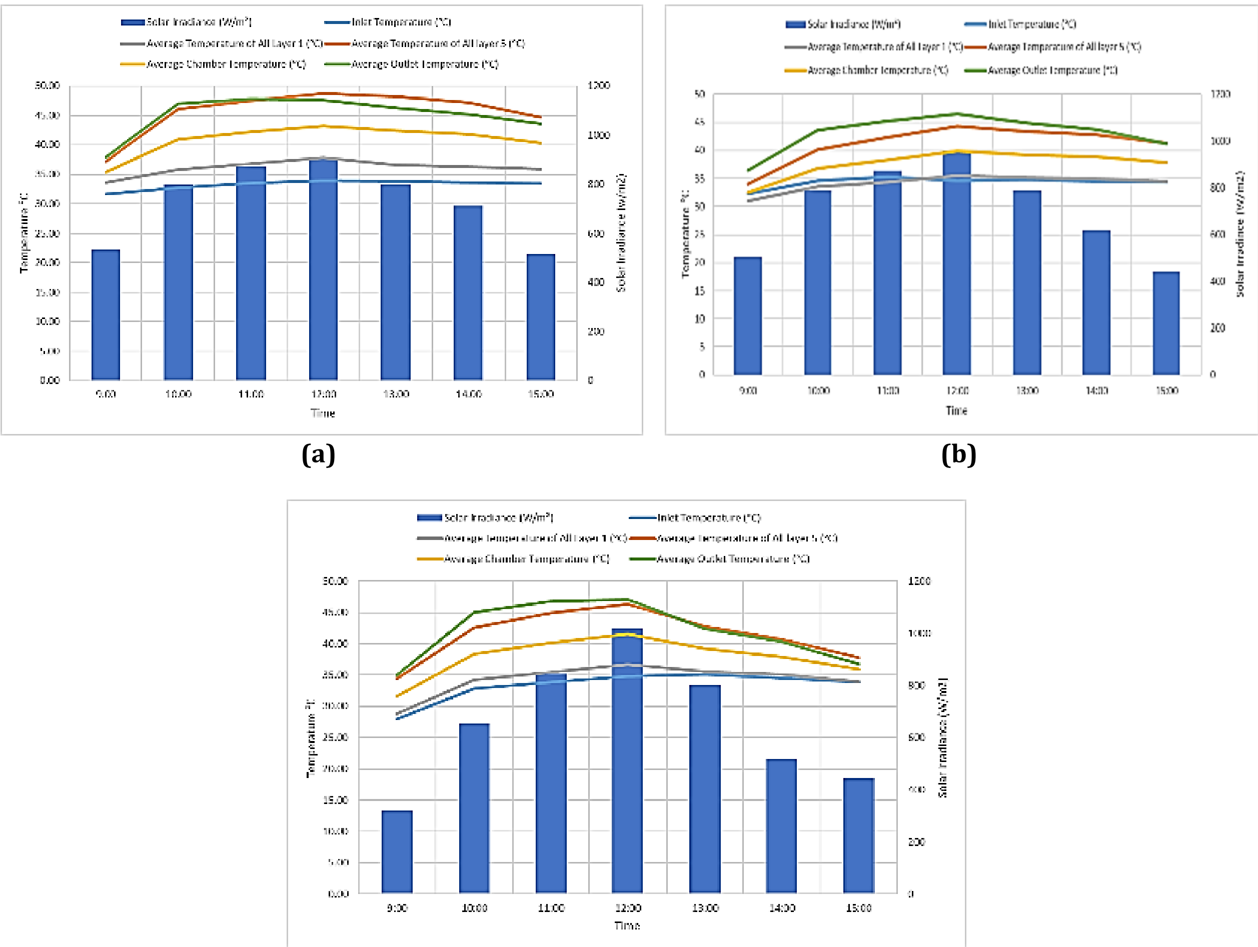

(a) (b) (c)

Fig. 6 *Temperature and solar radiation profiles across all experimental days (a) Day 1; (b) Day 2; (c) Day 3*

Based on the results obtained, a comparative analysis of the three days of the passive solar drying experiment reveals that the average solar irradiance on day 1 was 734 W·m^{-2}, approximately 3% higher than that on day 2 and 12% higher than that on day 3. The corresponding increase in solar irradiance on day 1 resulted in the highest mean temperature (43.25 °C), and the maximum vertical temperature difference was 15.07 °C between the inlet and the outlet. Additionally, there was a 7.25 °C temperature difference between layers 1 and 5. The 5-inch distance between the sponges enabled better airflow through each tray, thereby enhancing convective heat transfer and achieving a more uniform temperature distribution. On day 2, the average temperature decreased to 40 °C, and the temperature difference between the ambient and outlet decreased to 13 °C. Moreover, there was a 5.50 °C temperature difference between tray 1 and tray 5. These results indicate that there was less vertical temperature transfer on day 2. On day 3, the temperature differences were higher than those on day 2, at 17.52 °C and 7.64 °C, with an average temperature of 41.52 °C. The solar irradiance on day 3 was approximately 8% lower than that on day 2. The distance between the sponges, which is 1 inch between layers 5 and 1, restricted airflow through each tray, thereby leading to temperature accumulation near the upper layers and creating a significant temperature gradient. These results suggest that the temperature distribution is affected not only by solar irradiance but also by airflow characteristics, which are influenced by the spacing between the sponges. A larger spacing between the sponges enhances convective heat transfer and upward heating, whereas a smaller spacing constrains airflow and enhances temperature stratification.

3.2.2 Moisture Ratio (MR) Variation

The moisture ratio (MR) for all trays decreased progressively from morning to afternoon as shown in Fig. 7, indicating effective moisture removal over time. The top tray exhibited the fastest drying rate, with MR dropping from 1.000 to 0.161 by 3:00 PM. This is due to higher solar exposure and stronger airflow at the upper section. The middle tray followed with a final MR of 0.345, while the bottom tray dried slowest, reaching 0.377. This behaviour is likely due to lower heat penetration and limited air circulation near the chamber base.

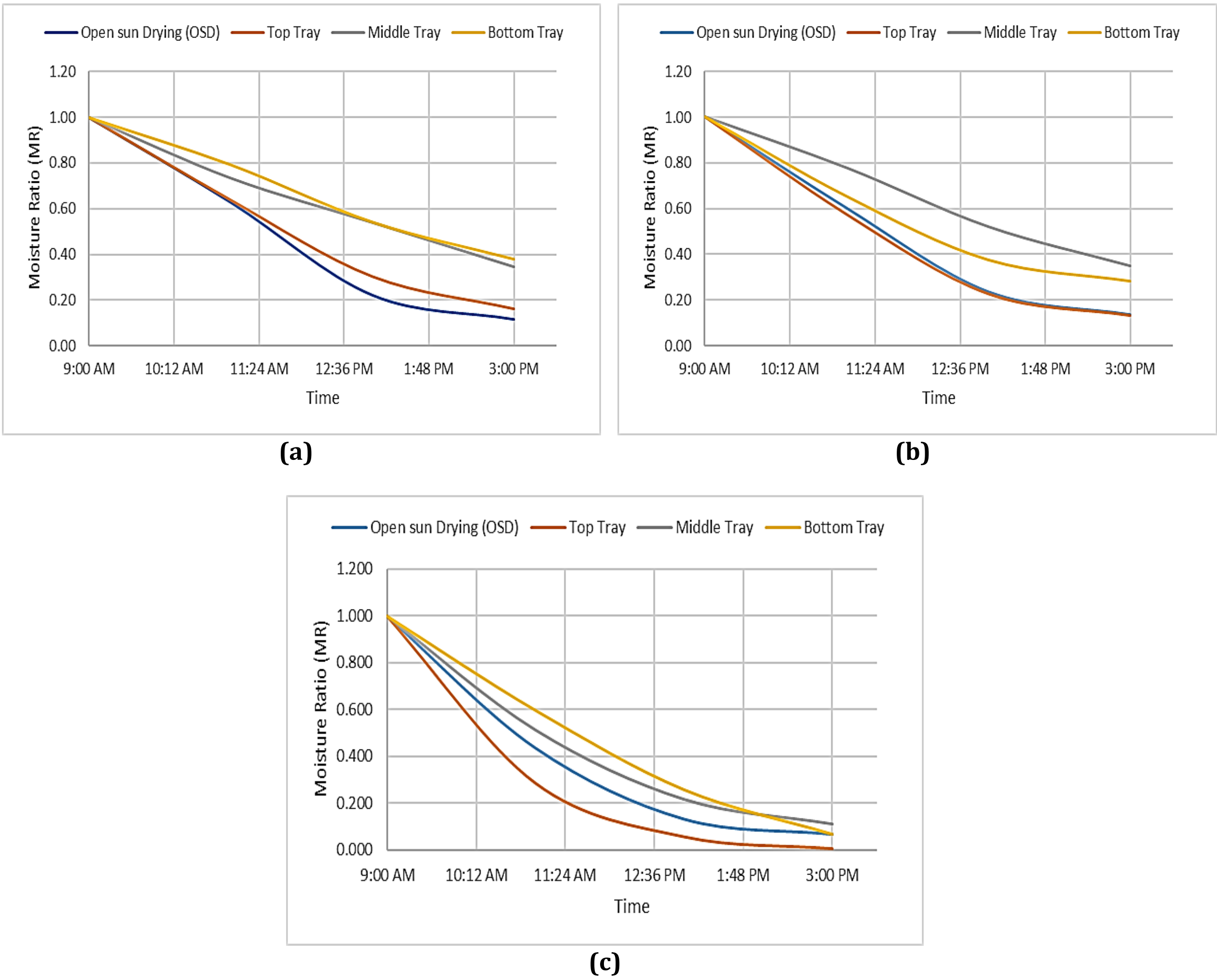

Fig. 7 *Moisture removal trends across trays across all experimental days (a) Day 1; (b) Day 2; (c) Day 3*

In comparison, open sun drying achieved an MR of 0.114, showing slightly faster drying because of direct solar radiation and unrestricted airflow. Comparing the area of open sun with tray instead of footprint of column, open sun drying showed highest moisture removal efficiency. Day 2, top tray recorded the fastest drying within the solar dryer, with MR reducing from 1.000 to 0.131 by 3:00 PM. Top Tray removed higher percent of water and this surpass the open sun drying BY 0.007 reducing from 1 to 0.14. This can be attributed to higher heat exposure and stronger airflow at the upper section. The middle tray showed moderate drying efficiency with MR declining to 0.348, while the bottom tray dried more slowly, reaching 0.284. Such behavior suggests reduced convective heat transfer near the chamber base due to higher sponge density and smaller air gaps. On day 3, the moisture ratio (MR) values showed a clear and steady decline across all trays throughout the drying period, indicating effective moisture removal. The middle tray followed by bottom and top have achieved the fastest drying, with MR decreasing dramatically from 1.000 to 0.110 ,0.067 0.004, by 3:00 PM and OSD decrease to final MR = 0.069.

The drying performance reflects the combined influence of solar irradiance and the distance between sponges on each tray. On Day 1, with the highest average irradiance (734 W·m^2) and widest spacing (5 in), the chamber reached its highest mean temperature (43.25 °C) and a vertical temperature difference of about 15 °C. Despite favorable heating, the moisture removal efficiency was lower than open-sun drying (OSD), particularly for the middle (−23 %) and bottom (−26 %) trays. This indicates that wide spacing enhanced airflow and reduced humidity buildup which allows heat to escape before sufficient vapor diffusion occurred. On Day 2, the average irradiance dropped slightly to 711 W·m^2, and spacing was reduced to 3 in. The average chamber temperature fell to 40 °C, and the temperature gradient narrowed to 13 °C.

Furthermore, the top tray performed comparably to OSD (+0.9 %), but the middle and bottom layers remained significantly lower (−21 % and −14 %), this indicate that moderate spacing still limited vertical heat transfer and retained moisture at lower levels. By contrast, day 3, despite lowest irradiance (657 W·m^2) and 1 inch spacing, produced stronger temperature stratification ($\Delta T \approx 17$ °C) but nearly uniform drying across all trays. The top layer achieved ≈ 99 % moisture removal, while the middle and bottom reached 89-93 %, approaching equilibrium with the upper layer. The nearly uniform MR on Day 3, despite pronounced stratification, is attributed to reduced convective escape paths under 1 inch spacing. This restriction increased vapor residence time and elevated local vapor pressure. Thus, it strengthens diffusive mass transfer independent of tray height. Consequently, the drying process became governed less by bulk airflow and more by internal vapor diffusion and boundary-layer thinning. It enables uniform moisture removal even when the temperature field remained strongly layered.

The drying uniformity inside the solar dryer was further evaluated using the standard deviation (SD) of moisture ratio (MR) values obtained from different tray levels. Lower SD values indicate more uniform drying conditions across the trays. As shown in Fig. 8, Day 3 exhibited the lowest SD values during the later stages of drying particularly at 3:00 PM (SD = 0.053). This observation suggests a more uniform moisture removal throughout the drying chamber, resulting in enhanced heat and airflow distribution within the dryer during the third experimental day.

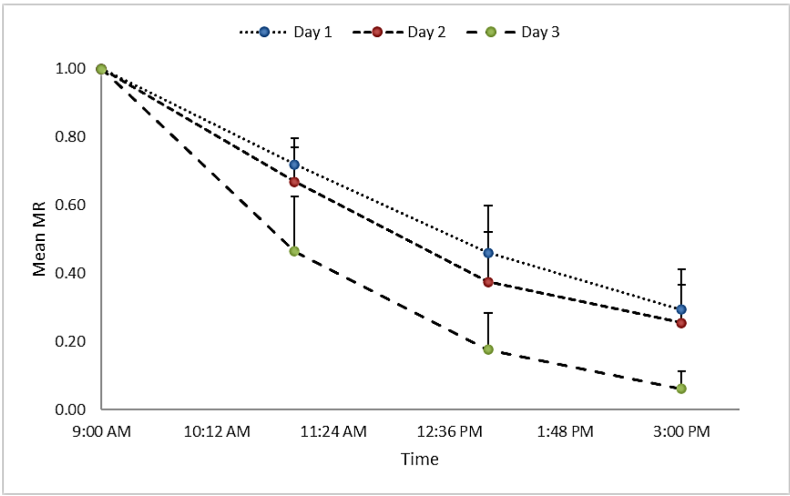

Fig. 8 *Mean moisture ratio (MR) versus drying time for three experimental days: Error bars represent ± standard deviation from different tray levels*

The closer sponge arrangement restricted airflow, increasing vapor residence time and enhancing overall drying intensity despite reduced solar input. These results reveal that drying behaviour depends not only on irradiance but also on internal airflow pathways. Wider spacing promotes more even temperature distribution but lower and uneven moisture removal, whereas narrow spacing increases localized heating and process reached to equilibrium, nearly uniform moisture removal. Hence, optimizing the sponge arrangement is crucial for balancing convective heat transfer and moisture diffusion within the drying chamber.

3.2.3 Drying Rate (DR) Variation

On day 1, the solar dryer recorded the highest mean solar irradiance of around 734 W/m^2, which correlated with the highest passive drying performance. For instance, the top tray recorded the highest drying rate of 0.16 kg/h, followed by the bottom tray with a drying rate of 0.11 kg/h. On the other hand, the lowest drying rate was recorded by the middle tray with a rate of 0.09 kg/h. Open sun drying recorded a comparable rate of 0.13 kg/h. On day 2, the solar irradiance reduced to 711 W/m^2, resulting in a moderate reduction in drying rates. For instance, the top tray recorded the highest drying rate of 0.14 kg/h and was in close proximity to the OSD rate of 0.13 kg/h. On the other hand, the bottom and middle trays recorded drying rates between 0.08 and 0.10 kg/h. On day 3, solar irradiance reduced to 657 W/m^2; however, drying rates became more uniform in all trays. For instance, the top tray, middle tray, and bottom tray recorded comparable mean drying rates of 0.09-0.11 kg/h. These rates were comparable with the OSD rate of 0.10 kg/h. Although the 1-inch spacing between sponge layers limited airflow, it reduced convective heat losses and enabled accumulation of heat in the chamber. This resulted in uniform drying rates despite reduced solar intensity. This pattern is illustrated in Fig. 9.

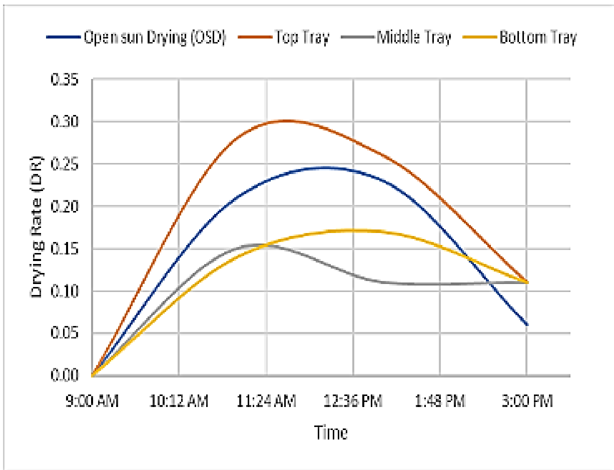

(a)

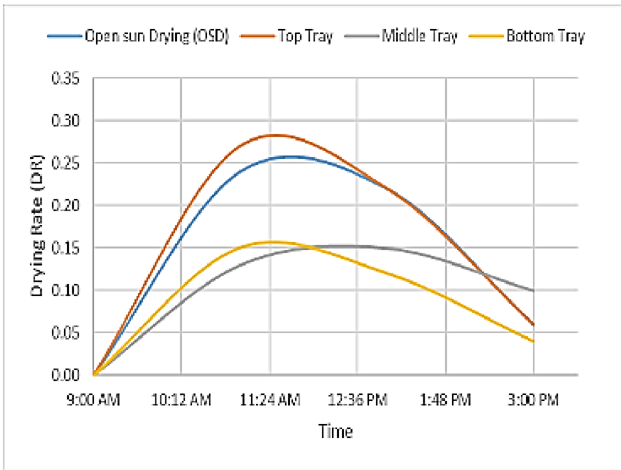

(b)

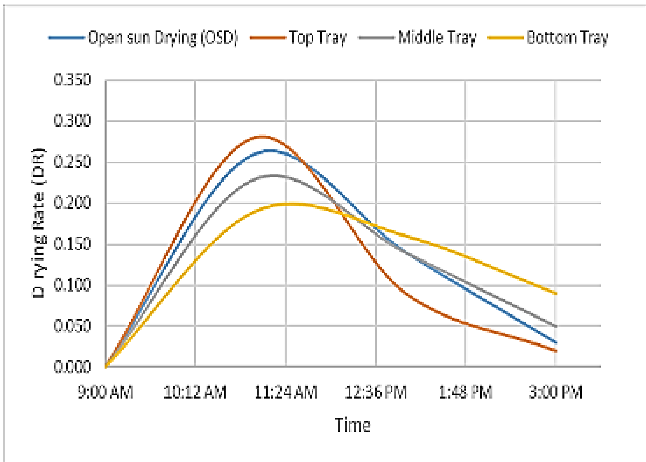

(c)

Fig. 9 *Drying rate trends (a) Day 1; (b) Day 2; (c) Day 3*

Two findings emerge. Firstly, higher irradiance resulted in higher peak rates (on Day 1, the top tray). However, as irradiance decreased from Day 1 to Day 3 (approximately 10–12%), the differences between trays narrowed. The top–bottom gap contracted from ≈ 0.05 kg h^{-1} to ≈ 0.01–0.02 kg h^{-1}, indicating progressively more balanced conditions. Second, thermal data clarify the mechanism. Day 1 showed a smaller vertical temperature gradient (ΔT ≈ 7–15 °C) with faster yet less uniform drying. Day 3 exhibited stronger stratification (ΔT ≈ 8–17 °C) but nearly even moisture removal (≈ 99% ± 1%). The 1-inch inter-sponge spacing likely restricted bulk airflow reduced convective heat loss, and increased vapor residence time, shifting control toward internal diffusion processes and boundary-layer effects rather than absolute irradiance. This interpretation aligns with porous-media drying theory, where the balance between convection and diffusion governs kinetics as the process transitions from early to later stages. A 100 W m^{-2} change in irradiance corresponded to an ≈ 2 ± 0.3 °C shift in chamber air temperature and an ≈ 8–12% change in moisture-removal efficiency, contingent on airflow resistance and spacing. This behavior demonstrates that wider spacing improves throughput but poses a risk of vertical non-uniformity. Conversely, tighter spacing promotes uniformity by retaining heat and vapor, albeit at the expense of some convective capacity (21).

3.2.4 Drying Efficiency Evaluation

The results for the total drying efficiency are presented in Table 2, where it is evident that the passive greenhouse solar dryer has much higher efficiency compared to OSD for all sponge loading conditions. This further confirms the advantage of the enclosed system in conserving thermal energy and promoting mass transfer. Table 1 has been designed to present a comprehensive comparison of the performance of the solar dryers, highlighting the effect of solar irradiance, sponge spacing, and sponge loading on the total thermal efficiency of the passive greenhouse solar dryer. On Day 1, the solar dryer had the highest efficiency of 86.25%, corresponding to 12 sponge loads and a 5-inch gap between them, owing to the high irradiance of 734 W/m^2 and good airflow, thus promoting robust convective heat transfer. Despite the presence of a steep vertical temperature gradient, the wider sponge spacing ensured rapid moisture removal of 1.44 kg, thus ensuring the full utilization of solar energy. On Day 2, the efficiency of 76.66% for 15 sponge loads per tray, corresponding to a 3-inch gap, is low despite the low irradiance loss of 3.1%, due to restricted convective heat transfer caused by the close sponge packing.

On Day 3, despite low irradiance of 656.65 W/m^2, the 1-inch sponge spacing configuration maintained the solar dryer efficiency at 83.67% for 15 sponge loads per tray, owing to the low convective heat loss within the solar chamber. This study thus clearly indicates that solar irradiance plays a critical role in determining the total solar energy available for drying, while the sponge spacing affects the efficiency of solar energy utilization for moisture removal. Under high solar irradiance, wider sponge spacing of about 5 inches ensured optimal utilization of solar energy, while under low solar irradiance, closer sponge packing of about 1 inch ensured optimal efficiency stability.

Table 2 *An Overall drying efficiency*

Day	Mode	Distance between sponge	Loading (sponges/tray)	Water removed (kg)/6 hour	Avg. solar (W/m^2)	Drying area (m^2)	Efficiency (%) dryer vs OSD
1	Dryer	5 inches	12	1.44	733.85	0.91	86.25
	OSD	5 inches		0.5			29.95
2	Dryer	3 inches	15	1.24	711		76.66
	OSD	3 inches		0.52			32.15
3	Dryer	1 inch	18	1.25	656.65		83.67
	OSD	1 inch		0.43			28.78

Across days, the passive greenhouse efficiencies (76.66–86.25%) surpass typical natural convection passive ranges reported in a large review (≈20–30% common; upper cases ≈49.5%), indicating performance near the best documented passive designs [25]. Compared with hybrid/forced systems, these values remain lower than the high efficiencies often achieved when auxiliary heating/forced convection and storage are employed, but they fall within the upper tier of passive only operation highlighted by recent syntheses [25], [26]. For cross study benchmarking, hybrid exemplars frequently report superior normalized performance (e.g., higher SMER); for instance, a PV assisted hybrid dryer achieved SMER ≈0.27 kg kWh^{-1} with substantially reduced SEC versus mixed mode/tray dryers (Jha and Tripathy, 2024, Results). Taken together, these comparisons suggest that the enclosure and load spacing strategy delivers passive efficiencies approaching optimized natural convection limits, while hybridization would be expected to enhance normalized metrics further [26].

4. Conclusions

The passive greenhouse solar dryer achieved substantially higher drying efficiencies (76–86%) than open-sun drying (≈30%), demonstrating its effectiveness as a controlled, energy-free drying system. The study showed that drying performance was strongly influenced by the interaction between solar irradiance, vertical temperature gradients, and tray-level inter-sponge spacing-directly addressing the objective of evaluating load-density and spacing effects on dryer behavior. Wider inter-sponge spacing (5 inches) enhanced convective airflow and increased chamber temperatures but resulted in uneven moisture removal due to rapid vapor escape. In contrast, the narrow 1-inch spacing restricted airflow, increased vapor residence time, and elevated internal heat retention, enabling highly uniform drying (≈99% moisture removal) even under lower irradiance. These findings confirm that optimizing inter-sponge spacing is critical for balancing convective heat transfer and moisture diffusion, and they validate the role of the T-shape configuration in supporting buoyancy-driven circulation.

In the context of larger-scale and industrial-scale applications, it is noted that the airflow limitations under dense loading conditions suggest that low-energy fan-assisted extraction at roof outlets (0.4-0.6 $m^3 s^{-1}$) and gentle cross-flow augmentation (0.2-0.3 $m^3 s^{-1}$ per column) can be beneficial in maintaining uniform airflow and moisture removal beyond natural convection capability. In terms of economics, it is noted that artificial convective drying processes require constant fuel and electricity supplies to facilitate hot air flow and drying, while the greenhouse passive dryer has zero energy costs, resulting in significantly lower life cycle cost per kilogram of removed water, especially under tropical conditions where high solar irradiance is available throughout the day. The porous open cell structure of the surrogate material is similar to crops with similar moisture transport characteristics, including leafy herbs (basil, mint), fruits (banana slices, apple chips), and vegetables (okra, mushroom slices). These crops are therefore strong candidates for future experiments using actual crops under similar airflow and thermal conditions.

For future work, experiments should be extended over multi-day experiments using actual crops and exploring hybrid and fan-assisted configurations to enhance scalability, robustness, and flexibility under various climatic conditions. Although surrogate materials, synthetic sponges, have been adopted in this work due to their regular geometry and consistent moisture characteristics, future experiments using actual crops can be extended to validate and explore similar airflow and thermal conditions. Based on this airflow pattern, future work can be extended to explore hybrid and fan-assisted configurations, as well as economic viability to enhance commercialization.

Acknowledgement

The authors wish to convey sincere gratitude to Universiti Malaysia Sabah (UMS) and Ministry of Higher Education (MOHE) for supporting the current research work thru UMS research grant, GUG0696 and IMAP004-2/2024.

Conflict of Interest

The authors declare that they have no known financial, personal, or institutional conflicts of interest that could have influenced the work reported in this manuscript.

Author Contribution

*The authors confirm contribution to the paper as follows: **study conception and design**: Mohd Suffian Misaran, Chu Chi Ming, Md Mizanur Rahman; **data collection**: Abdul Rahman, Mohd Kamel Wan Ibrahim, Mohd Adzrie Radzali; **analysis and interpretation of results**: Abdul Rahman, Mohd Suffian Misaran, Chu Chi Ming, Tham Heng Jin, Rachel Fran Mansa; **draft manuscript preparation**: Abdul Rahman, Md Mizanur Rahman, Mohd Suffian Misaran, Chu Chi Ming. All authors reviewed the results and approved the final version of the manuscript.*

References

[1] Y. E. Maryana, D. Saputra, G. Priyanto & K. Yuliati (2023, November 8-9). *A review of the inflated solar dryer for improving the quality of agricultural product* [IOP Conference Series: Earth and Environmental Science]. Padang, Indonesia, *1160(1)*, 012075, https://doi.org/10.1088/1755-1315/1160/1/012075

[2] Jasmine Petikirige, Azharul Karim & Graeme Millar (2022) Effect of drying techniques on quality and sensory properties of tropical fruits, *International Journal of Food Science & Technology*, *57(11)*, 6963-6979, https://doi.org/10.1111/ijfs.16043

[3] Abdulrahim, Al-Ismaili (2025) A review on solar drying of fish, *Journal of Agricultural and Marine Sciences*, *26(2)*, 1-9, https://doi.org/10.53541/jams.vol26iss2pp1-9

[4] Decheng Kong, Yunfeng Wang, Ming Li, and Jingkang Liang (2024) A comprehensive review of hybrid solar dryers integrated with auxiliary energy and units for agricultural products, *Energy*, *293*, 130640, https://doi.org/10.1016/j.energy.2024.130640

[5] Rohit Kumar Yadav (2023) Comparative overview of performance of the dryers with a conventional method of drying i.e., open sun drying, *International Journal of Environment and Climate Change*, *13(9)*, 383-387, https://doi.org/10.9734/ijecc/2023/v13i92244

[6] Theeraphan Chumroenphat, Ananya Dechakhamphu, Surapon Saensouk & Sirithon Siriamornpun (2025) Drying conditions affected chemical profiles and health promoting properties of Castanopsis piriformis Hickel & A.Camus, *Food Chemistry: X*, *29*, 102874, https://doi.org/10.1016/j.fochx.2025.102874

[7] Sumit Kumar Verma, P. Ganesan, Pankaj Kishor, CO Remya Sasikala, P. P. Mohan, N. Muralidharan & B. Jagannath (2024) Effect of microwave and conventional drying process on the drying kinetics and physico-chemical quality of brown shrimp (Metapenaeus dobsonii): Advanced Microwave drying on the quality of shrimp, *Indian Journal of Fisheries*, *71(2)*, 105-122, https://doi.org/10.21077/ijf.2024.71.2.139441-14

[8] Ohood Al-Ghadani, Mawada Al-Khayari, Hemanatha Jayasuriya, Pankaj B. Pathare & Mohammed Al-Belushi (2024) Drying characteristics and kinetics of bottle gourd using stand-alone indirect solar dryer, *Frontiers in Sustainable Food Systems*, *8*, 1400938, https://doi.org/10.3389/fsufs.2024.1400938

[9] Florence M. Mashitoa, Tinotenda Shoko, Jerry L. Shai, Retha M. Slabbert, Yasmina Sultanbawa & Dharini Sivakumar (2021) Influence of different types of drying methods on color properties, phenolic metabolites and bioactivities of pumpkin leaves of var. Butternut squash (Cucurbita moschata Duchesne ex Poir). *Frontiers in Nutrition*, *8*, 694649, https://doi.org/10.3389/fnut.2021.694649

[10] Necati Çetin & Cevdet Sağlam (2023) Effects of ultrasound pretreatment assisted drying methods on drying characteristics, physical and bioactive properties of windfall apples, *Journal of the Science of Food and Agriculture*, *103(2)*, 534-547, https://doi.org/10.1002/jsfa.12164

[11] Onyinyechi Nnamchi, Cyprian Tom, Godwin Akpan, Murphy Umunna, David Ubong, Mathew Ibeh, Adindu Linus–Chibuezeh, Leonard Akuwueke, Stephen Nnamchi, Augustine Ben & Macmanus Ndukwu (2025) Solar dryers: A review of mechanism, methods and critical analysis of transport models applicable in solar drying of product. *Green Energy and Resources*, *3(2)*, 100118, https://doi.org/10.1016/j.gerr.2025.100118

[12] Sadaf Gul Unar, Shoaib Ahmed Khatri, Nayyar Hussain Mirjat, Pervez Hameed Shaikh, Syed Abdul Rafay Ahmed Zaidi & Muhammad Faraz Arain (2026) Solar drying technologies: A review of design, efficiency, and environmental impacts, *Renewable and Sustainable Energy Reviews*, *226*, 116339, https://doi.org/10.1016/j.rser.2025.116339

[13] Samuel Ayofemi Olalekan Adeyeye, Tolulope Joshua Ashaolu & Ayenampudi Surendra Babu (2022) Food Drying: A Review, *Agricultural Reviews*, *1(8)*, 1-8, https://doi.org/10.18805/ag.R-2537

[14] James Menya, Kant Kanyarusoke & Wilson Babu Musinguzi (2024) Solar food/crop drying practices in Uganda: The state of the art & prospective development, *International Journal of Scientific Advances*, *5(2)*, https://doi.org/10.51542/ijscia.v5i2.25

[15] Jasinta Poonam Ekka & Muthukumar Palanisamy (2020) Determination of heat transfer coefficients and drying kinetics of red chilli dried in a forced convection mixed mode solar dryer, *Thermal Science and Engineering Progress*, *19*, 100607, https://doi.org/10.1016/j.tsep.2020.100607

[16] Md Atiqur Rahman, SM Mozammil Hasnain, Prabhu Paramasivam, Rustem Zairov & Abinet Gosaye Ayanie (2025) Solar drying for domestic and industrial applications: A comprehensive review of innovations and efficiency enhancements, *Global Challenges*, *9(2)*, 2400301, https://doi.org/10.1002/gch2.202400301

[17] Pushpendra Singh & M. K. Gaur (2021) Sustainability assessment of hybrid active greenhouse solar dryer integrated with evacuated solar collector, *Current Research in Food Science*, *4*, 684-691, https://doi.org/10.1016/j.crfs.2021.09.011

[18] Ch Nettari, A. Boubekri, A. Benseddik, S. Bouhoun, D. Daoud, A. Badji & I. Hasrane (2024) Design and performance evaluation of an innovative medium-scale solar dryer with heat recovery based-latent heat storage: Experimental and mathematical analysis of tomato drying, *Journal of Energy Storage*, *88*, 111559, https://doi.org/10.1016/j.est.2024.111559

[19] Phatcharapron Sukkanta, Kornkanok Eiamkij, Nachason Junset & Krittaphas Mongkoldhumrongkul (2023) Oyster mushroom drying efficiency using a solar dryer, *Energy Reports*, *9*, 479-486, https://doi.org/10.1016/j.egyr.2023.01.062

[20] Hossein Chaji, Parvin Sharayei, Mahdi Hedayatizadeh, Yeganeh Sabeghi & Danial Gandomzadeh (2024) Drying kinetics and quality attributes of solar-dried red peppers: A comparative study with traditional and industrial methods, *Journal of Food Processing and Preservation*, *2024*, 1-11, https://doi.org/10.1155/2024/7987269

[21] Stephen Whitaker (1977) Simultaneous heat, mass, and momentum transfer in porous media: A theory of drying, In *Advances in Heat Transfer*, *13*, 119-203, https://doi.org/10.1016/S0065-2717(08)70223-5

[22] Ellen K. Luckins (2025) Mathematical modelling of drying capillary porous media, *Journal of Fluid Mechanics*, *1017*: A6, https://doi.org/10.1017/jfm.2025.10432

[23] Jungchul Kim, Jonghyun Ha & Ho-Young Kim (2017) Capillary rise of non-aqueous liquids in cellulose sponges, *Journal of Fluid Mechanics*, *818*, R2, https://doi.org/10.1017/jfm.2017.165

[24] Jonghyun Ha, Jungchul Kim, Yeonsu Jung, Giseok Yun, Do-Nyun Kim & Ho-Young Kim (2018) Poro-elasto-capillary wicking of cellulose sponges. *Science Advances*, *4(3)*, eaao7051, https://doi.org/10.1126/sciadv.aao7051

[25] Mfanafuthi Mthandeni Mkhize (2025) Review of solar crop drying efficiency and its interconnection with meteorological factors, *Discover Energy*, *5(1)*, 22, https://doi.org/10.1007/s43937-025-00088-2

[26] Kavati Venkateswarlu & SV Kota Reddy (2024) Recent trends on energy-efficient solar dryers for food and agricultural products drying: A review, *Waste Disposal & Sustainable Energy*, *6(3)*, 335-353, https://doi.org/10.1007/s42768-024-00193-3